Soft Matter

PAPER

View Article Online
View Journal

Cite this: DOI: 10.1039/d1sm00221j

Enzymes hosted in redox-active ionically cross-linked polyelectrolyte networks enable more efficient biofuel cells†

Lucy L. Coria-Oriundo, [ab] M. Lorena Cortez, [c] Omar Azzaroni *[c] and Fernando Battaglini *[a]

Received 11th February 2021,
Accepted 23rd April 2021

DOI: 10.1039/d1sm00221j

rsc.li/soft-matter-journal

Redox mediators are pivotal players in the electron transfer process between enzymes and electrodes. We present an alternative approach for redox mediation based on branched polyethyleneimine (BPEI) modified with an osmium complex. This redox polyelectrolyte is crosslinked with phosphate to produce colloidal particles with a diameter of *ca.* 1 μm, which, combined with glucose oxidase (GOx), can form electroactive assemblies through either layer by layer assembly (LbL) or one-pot drop-casting (OPDC). The addition of NaCl to these colloidal systems induces the formation of films that otherwise poorly grow, presenting an outstanding catalytic current. The system was tested as a bioanode delivering a power output of 148 μW per nmol of mediator. These results are explained in terms of the interactions of the ions with the polyelectrolyte and represent a new route for the development of bioelectrochemical devices involving redox mediators and enzymes.

1 Introduction

Ionically crosslinked polyelectrolyte micro- and nanoparticles are materials prepared by combining polyelectrolyte chains with multivalent ions. Of these materials, polyamine/salt colloids have been extensively studied, where multivalent anions trigger the spontaneous self-assembly of the polyamine given a stable colloidal suspension.[1–5] Among these systems, those based in chitosan or polyallylamine are the best characterized. More recently, branched polyethyleneimine (BPEI) was incorporated into the set of crosslinked polyamines combined with ferrioxalate as a responsive material.[6]

Polyethyleneimine is a positively charged polyelectrolyte widely used in enzyme immobilization.[7] Its success is due to several features such as chemical structure, solubility, and charge density, among others. It can be obtained in linear, branched, comb, network, and dendrimer architectures depending on the synthetic route. BPEI presents primary, secondary, and tertiary amino groups with different pKa,[8] which introduces different options regarding further reactions and molecular interactions. In contrast to polyallylamine or chitosan, it is soluble in a broad range of solvents.[9] As the molecular weight of its monomer unit is 43, the charge density is higher than other positively charged polyelectrolytes.

On the other hand, several applications related to the combination of PEI with redox enzymes can be found in the literature; for example, ferrocene modified linear PEI was combined with glucose oxidase (GOx) as bioanode in LbL built electrodes.[10–13] Recently, BPEI was modified with ferrocene and introduced in nanobeads to construct glucose biosensors.[14] More complex constructions include the incorporation of carbon nanotubes[15,16] or gold nanoparticles.[17] Even though ferrocene derivatization is a fast and straightforward method, the resulting product presents some limitations; for example, its stability in the oxidized form is limited, and its redox potential is too high for several applications.[11]

Chain conformation in polyelectrolytes is strongly influenced by pH, ionic strength, and the type of ions present in the solution. These properties can be exploited to integrate protein to assemblies independently of its charge[18,19] or improve its electrochemical response, as we have recently shown with polyallylamine and glucose oxidase.[20] Little is known about this influence on BPEI,[6] which is a very suitable polyelectrolyte.

[a] *INQUIMAE (CONICET), Departamento de Química Inorgánica, Analítica y Química Física, Facultad de Ciencias Exactas y Naturales, Universidad de Buenos Aires, Ciudad Universitaria, Pabellón 2, C1428EHA Buenos Aires, Argentina. E-mail: battagli@qi.fcen.uba.ar*

[b] *Facultad de Ciencias, Universidad Nacional de Ingeniería, Av. Túpac Amaru 210, Lima 25, Peru*

[c] *Instituto de Investigaciones Fisicoquímicas Teóricas y Aplicadas (INIFTA), Departamento de Química, Facultad de Ciencias Exactas, Universidad Nacional de La Plata, CONICET, Sucursal 4, Casilla de Correo 16, 1900 La Plata, Argentina. E-mail: azzaroni@inifta.unlp.edu.ar.web; Web: http://softmatter.quimica.unlp.edu*

† Electronic supplementary information (ESI) available. See DOI: 10.1039/d1sm00221j

In this work, we present the assembly of a redox BPEI with GOx manipulating the environment in which the buildup process is carried out. The redox moiety is a polypyridyl osmium complex (OsBPEI), providing a stable and reversible electron transfer process. At high ionic strength, given by NaCl, the presence of phosphate ions generates colloids that can build up interfacial nanoarchitectures, presenting an efficient electron transfer process. Layer-by-layer (LbL) and one-pot drop-casting (OPDC) self-assembly techniques were explored to establish the best way to generate a system able to produce an efficient electron transfer process, exemplified in its application as an anode in biofuel cells. The results presented here show the impact of variables as ionic strength and ion composition to control the nanoarchitecture of the assemblies and its redox response, simplifying the construction and improving bioelectrochemical devices' performance.

2 Experimental

Reagents, quartz crystal balance (QCM-D), electrochemical, and dynamic light scattering experiments are described in ESI.† $[Os(bpy)_2Cl(PyCOH)]Cl$ was synthesized following the procedure of Kober *et al.*[21] The complex was bound to the polyelectrolyte adapting the procedure of Danilowicz *et al.*[22] Details are given in ESI.† Electrode modifications: in-house constructed screen printed 3-electrode system with graphite or gold working electrodes were used.[23,24] Layer by layer electrode modification was carried out on gold working electrodes. OsBPEI was dissolved in a final osmium concentration of 0.48 mM in the matrices listed in Table 1, while 1 mg mL^{-1} glucose oxidase (GOx) was dissolved in water pH 7.0. The working electrodes were sequentially exposed to 15 μL of the OsBPEI and GOx solutions and left for 20 minutes in a closed container with controlled humidity (92% RH, controlled with a potassium nitrate saturated solution). Then, the electrodes were rinsed with Milli-Q water; finally, they were dried with a flux of nitrogen and used for the electrochemical experiments. For one-pot drop-casting experiments, graphite was used as the working electrode, while GOx was added to the OsBPEI solutions at a final concentration of 1 mg mL^{-1}; otherwise, it is stated. 10 μL of the corresponding solution was left to dry in a closed container with controlled humidity (30% RH, controlled with a saturated $CaCl_2$ solution) and then rinsed with water and dried with a nitrogen current. PEGDE crosslinking was carried out by adding to the matrix; the used concentrations are stated throughout the text.

Table 1 Nomenclature and composition of the solutions used in this work

Solution name	Solution composition[a]
1 M NaCl	1.00 M NaCl
1 mM Pi–NaCl	1.0 mM K_2HPO_4 + 1.00 M NaCl
10 mM Pi–NaCl	10 mM K_2HPO_4 + 1.00 M NaCl
1 mM Pi	1.0 mM K_2HPO_4
10 mM Pi	10 mM K_2HPO_4

[a] All solutions at pH = 7.0.

Nomenclature. For clarity, we employ the following shorthand to identify the different solutions used in the buildup process: X@Y; where X represents OsBPEI or GOx, and Y represents the medium where they are dissolved (Table 1); for example, OsBPEI@1 mM Pi–NaCl represents OsBPEI dissolved in a 1 mM phosphate solution in the presence of 1 M NaCl (second entrance in Table 1).

3 Results and discussion

As BPEI is readily soluble in methanol, its modification with a mediator bearing an aldehyde group was straightforward, yielding a redox polyelectrolyte containing one osmium complex every 16 amino groups. These results represent two advantages over a similar redox polyelectrolyte based on polyallylamine (PA), it is easier to handle, and the density of redox groups achieved here is higher.[20,25] Another feature to consider is its branched structure, presenting different amino groups, primary (terminals), secondary (backbone), and tertiary (ramification points) (see Fig. S2, ESI†). Studies on the PEI protonation established pseudo-acid dissociation constants (K′) based on the chemical shifts observed in the neighbor methylene groups by NMR.[8] In this way, it was determined that the primary amino groups are the first to be protonated, with a pK' of 9.4, while the tertiary amino groups cannot be protonated at pH above 0. The secondary amino groups, which constitute the polymer backbone, behave differently depending on their neighbors, with pK' values ranging from 8.6 to 4.4. Potentiometric titrations and NMR studies carried out on BPEI of different molecular weights have found that 30% or more of the amino groups cannot be titrated, representing a high number of tertiary amino groups meaning that most of these polymers are highly branched.[8,26] In our case, the potentiometric titration of the BPEI used in this work shows that 40% remains unprotonated, and 17% of the amino groups are protonated at pH 7 (see ESI† and Fig. S3).

Considering these features, we studied the OsBPEI under different conditions to manipulate its conformational state and determine to what extent the polyelectrolyte conformation affects the electron transfer process once assembled with GOx. Anions can interact with polymers and their hydration waters by different mechanisms: (a) polarizing adjacent water molecules, (b) increasing the surface tension around the polymer backbone, and (c) the anions may bind to the polymer. The two first effects lead to a salting-out process, while the last one leads to the salting in of the polymer.[27] Here, we study the effect of chloride and phosphate ions on the OsBPEI conformation in solution in different conditions: 1 M NaCl, 1 mM phosphate at pH 7.0, and the combination of 1 M NaCl and 1 mM phosphate at pH 7.0, also the polyelectrolyte in deionized water was studied as reference. Dynamic light scattering experiments in water and 1 M NaCl show that the polyelectrolyte presents sizes ranging from 0.5 to 5 nm, evidencing that it is unable to form a colloidal structure. When OsBPEI is dissolved in the presence of 1 mM phosphate forms colloidal particles in a bimodal distribution (730 and 1300 nm) and with a positive Z-potential (11 mV) (see Table 2),

Table 2 OsBPEI solutions studied by Dynamic Light Scattering (DLS)

Samples[a]	Diameter nm^{-1}	PDL	Zeta potential mV^{-1}
@1 M NaCl	0.5–5	1.0	4
@1 mM Pi	$(7.3 \pm 0.9) \times 10^2$	0.6	11
	$(1.3 \pm 0.1) \times 10^3$	0.3	
@1 mM Pi–NaCl	$(8.6 \pm 0.7) \times 10^2$	0.4	BAT[b]
@10 mM Pi	$(8 \pm 1) \times 10^2$	0.6	16
@10 mM Pi–NaCl	$(1.5 \pm 0.4) \times 10^3$	0.6	BAT[b]
@GOx,10 mM Pi–NaCl	$(1.5 \pm 0.2) \times 10^3$	0.5	BAT

[a] Nomenclature of the samples is given in Table 1 (Experimental section). [b] Below the acceptable threshold.

showing the ability of phosphate to interact with the amino groups through hydrogen bonds. Adding 1 M NaCl, a less disperse suspension is obtained with particles of 860 nm diameter. Cl^- ions' high concentration increases the surface tension around the polymer backbone and screens the interaction between phosphate ions and amino groups, leading to narrower particle size distribution.[28,29] Recently, the study of the physicochemical interactions between polyallylamine and phosphate ions was systematically addressed, varying the pH and the ionic strength of the solution.[2] The authors found that the driving force leading to the formation of colloids is the electrostatic paring of protonated amino groups and the HPO_4^{2-}, while the addition of a monovalent salt weakens this interaction, in agreement with previous works with chitosan.[28,29] BPEI presents a more complex structure with different types of alkylamino groups. The primary amino groups and part of the secondary amino groups are protonated at pH 7.0; therefore, they are the best candidates to interact with the phosphate ions. However, they represent less than 20% in contrast to linear polyallylamine and chitosan, thus promoting the bridging between phosphate groups and different BPEI molecules that, in turn, facilitates the construction of greater colloidal particles. Finally, in those cases where Z-potential was determined, a positive charge was observed due to the excess of amino groups. The Z-potential measurements are limited to relatively low ionic strength solutions (<0.1 M); when solutions have high ionic strength (*e.g.*, 1 M), the streaming potential signal shows values below the acceptable threshold for electrode polarization.[30,31]

From DLS results, we can assert the formation of self-limited assemblies in solution. They were combined with glucose oxidase to construct glucose-responsive electrodes through different strategies, layer by layer (Scheme 1A) and one-pot drop-casting (Scheme 1B); both techniques are carried out in mild conditions, representing a friendly environmental method of production.

One of the advantages of PEI to build self-assembled systems is its ability to bind directly on gold,[32–34] and avoid its previous modifications with thiol groups, representing a source of instability.

The layer by layer deposition of polyelectrolytes in the presence of small ions is a technique widely studied; depending

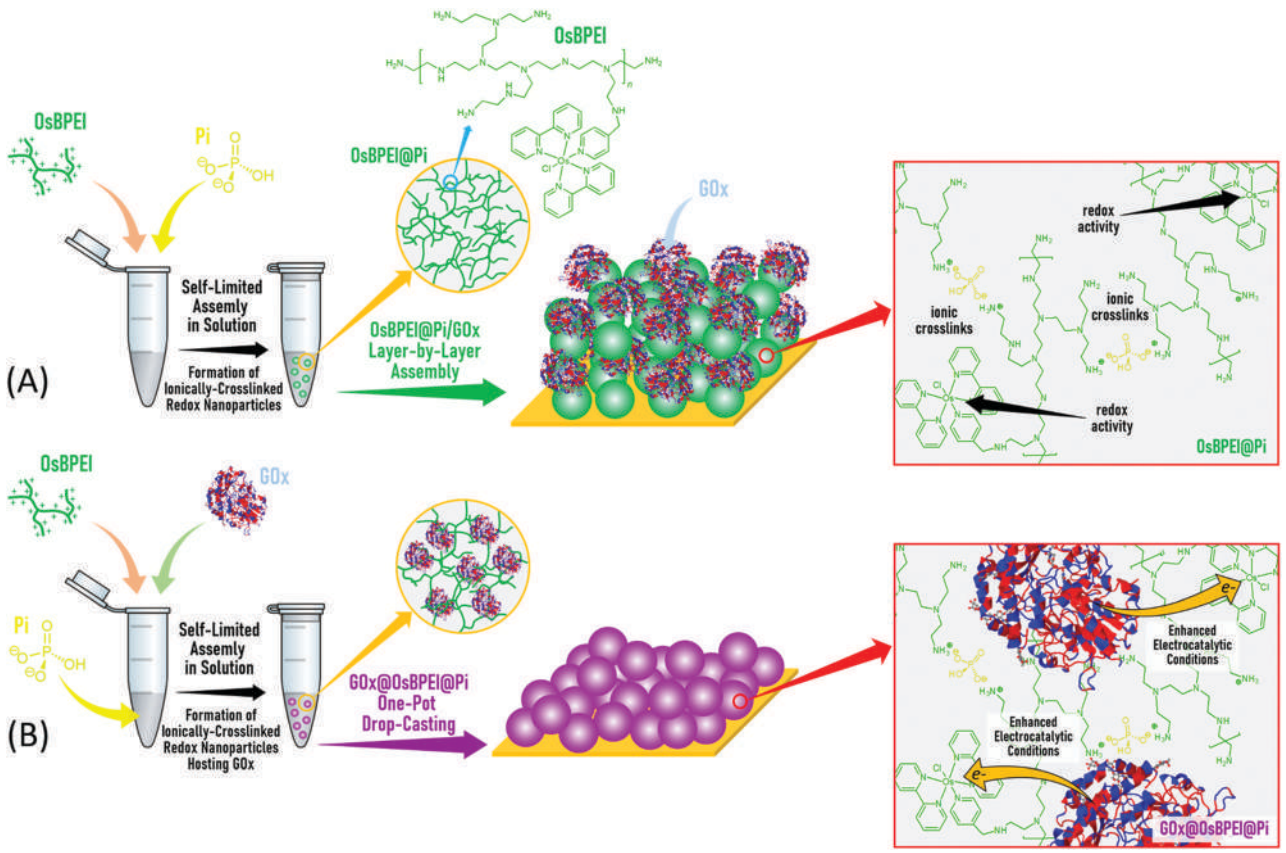

Scheme 1 Description of the electrode modification *via* different self-assembly processes: (A) layer-by-layer assembly, (B) one-pot drop-casting assembly.

on the type of ions and their concentration, different results can be achieved.[35–37] The interaction between phosphate ions and polyallylamine is an interesting example since the polyelectrolyte's primary amino groups can form hydrogen bridges with the phosphate groups.[38,39] Depending on the pH and the ionic strength, this interaction can contribute in different ways; for example, avoiding the further assembly of an enzyme at low ionic strength[35] or improving its adsorption at high ionic strength.[20]

Fig. 1 shows the current response for a film assembled by alternative OsBPEI and GOx layers at different conditions. The represented current densities correspond to the values obtained by cyclic voltammetry at 10 mV s^{-1}. In Fig. 1A the plotted values correspond to the peak currents in the absence of glucose, while for Fig. 1B, the values correspond to the catalytic current in the presence of 100 mM glucose.

We can observe that the OsBPEI/GOx assembly can be built from pure aqueous solutions and even at high ionic strength, in contrast to the observed with osmium derivatized polyallylamine (OsPA).[20] However, the ratio between the catalytic and the peak currents is around 4, showing that GOx is poorly incorporated into the film, or its connection to the OsBPEI is relatively weak. In the presence of phosphate, we observed that the adsorption of OsBPEI is possible. The current in the absence of glucose grows as the number of layers increase; however, in the presence of glucose, a poor catalytic process is observed. Finally, the higher currents are obtained when OsBPEI is assembled from a solution containing 1 mM phosphate and 1 M NaCl. In the absence of glucose, it is possible to observe a notable difference concerning the other construction methods, that it is enhanced in the presence of glucose where a catalytic current of 52 μA cm^{-2} is observed. A ratio equals to 19 is obtained between the current in the presence and in the absence of glucose (j_c/j_0), which is higher than those observed in LbL assemblies with GOx and other redox polyelectrolytes ($j_c/j_0 \approx 10$),[20,40] indicating that this construction allows a more efficient interaction between the redox centers, FAD in GOx and the osmium complex in PEI.

The growth of the system when OsBPEI is dissolved in pure water can be explained by the electrostatic interaction, while in

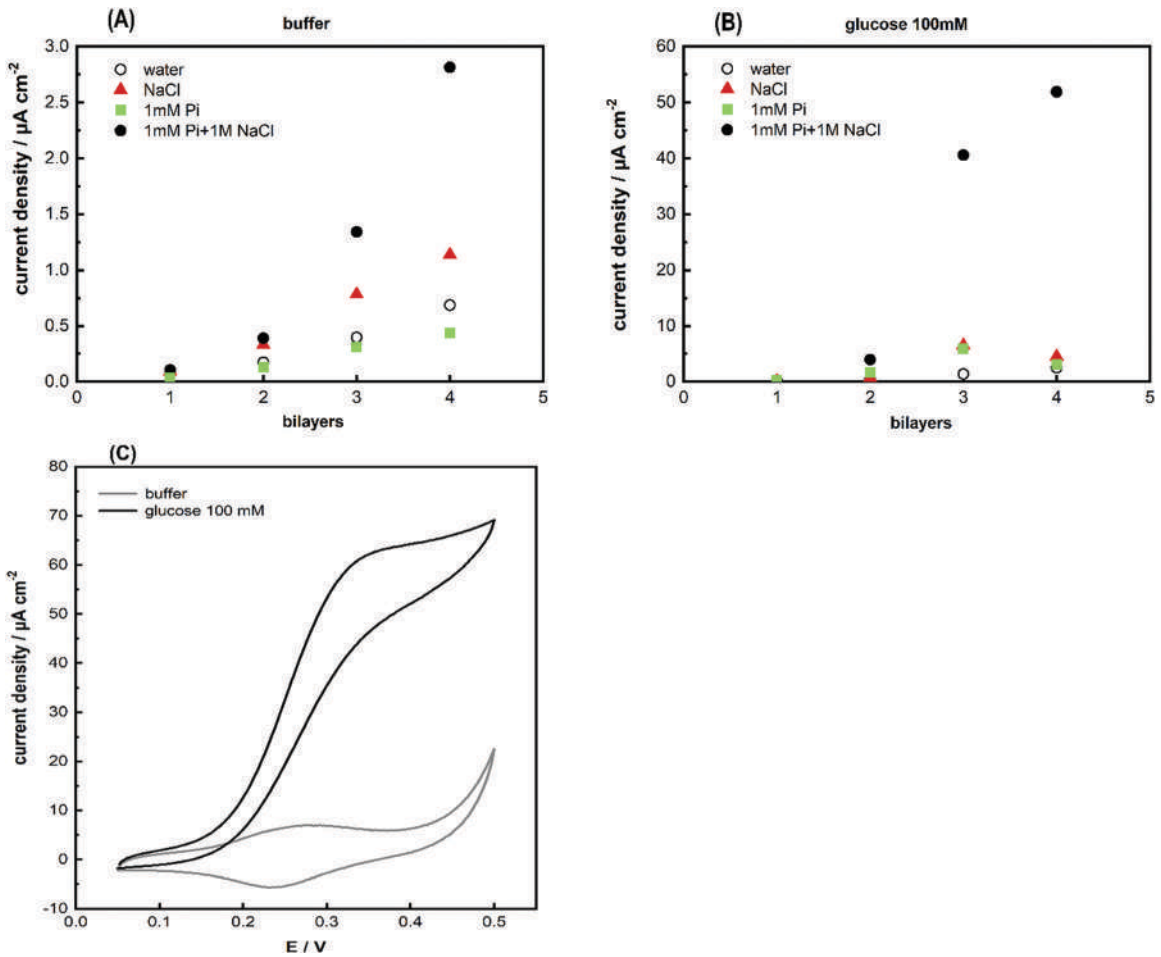

Fig. 1 (A) Peak current densities for cyclic voltammetries carried out at 10 mV s^{-1} after deposition of each bilayer (OsBPEI/GOx) on gold screen printing electrodes in the absence of glucose. (50 mM HEPES buffer + 0.1 M NaCl, pH = 7.0). (B) Maximum catalytic currents in the presence of 100 mM Glucose in 50 mM HEPES buffer + 0.1 M NaCl, pH = 7.0. (○) $(OsBPEI/GOx)_n@H_2O$, (▲) $(OsBPEI@1\ M\ NaCl/GOx@H_2O)_n$, (■) $(OsBPEI@1\ mM\ Pi/GOx@H_2O)_n$, (●) $(OsBPEI@1\ mM\ Pi–NaCl/GOx@H_2O)_n$. All solution at pH 7.0. (C) Cyclic voltammetries for $(OsBPEI@1\ mM\ Pi–NaCl/GOx@H_2O)_4$ in the presence of 100 mM glucose (black line) and the absence of glucose (grey line).

NaCl by a salting-out effect promoting van der Waals interactions. When phosphate is present in the solution, the polyelectrolyte in the film can be re-dissolved due to the competition between the phosphate already in the film and those in the solution, showing the poorest performance during the growth cycling (Fig. 1A, green squares). The introduction of NaCl to the phosphate solution produces a synergic effect. It promotes a salting-out effect due to the increase of the surface tension between the macromolecules and water.[27] Favoring the bridging of the phosphate ions in the film. This bridging effect is also known in proteins through the basic amino acid residues such as lysine and arginine, several of them in the periphery of the GOx. In this sense, phosphate ions have shown to be suitable promoters to stabilize several proteins onto electrodes due to their ability to interact with amino groups.[41–43] This ionic environment improves the interaction between the enzyme and the osmium mediator bound to the polyelectrolyte, notably evidenced by the catalytic current observed in this case (Fig. 1B and C).

At high ionic strength and in the presence of phosphate, QCM-D data show that the incorporation of OsBPEI and GOx in the film is similar (Fig. 2, frequency change, circles). While the dissipation change for OsBPEI, in each adsorption step, is around 5 times higher than for GOx (Fig. 2, squares), this is evidence of the gel-like structure of the OsBPEI particles compared with the more rigid and smaller structure of the protein. An immediate consequence of the OsBPEI:GOx ratio in the adsorbed mass is the number of redox centers surrounding the GOx, *ca.* 90 : 1, while in the case of OsPA is 10.[20]

We have demonstrated that OsBPEI can form microgels by ionic phosphate crosslinking, a behavior already observed in other amino-based polyelectrolytes.[29,35,44] Also, it can be observed that these colloidal particles in the presence of a high concentration of monovalent salts are stable, and they can be used in the buildup of the LbL system with GOx, showing an important effect on the electrochemical response.

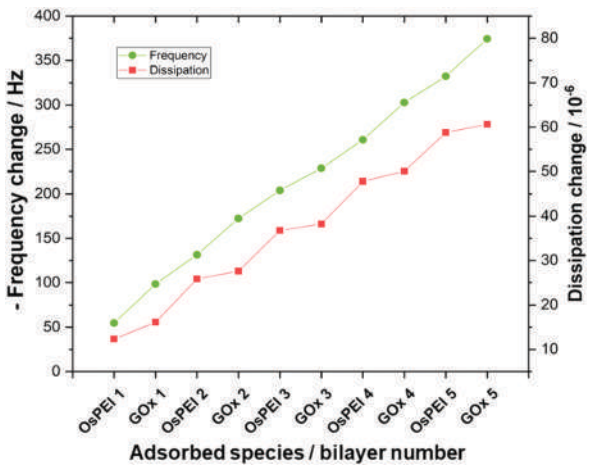

Fig. 2 QCM-D results for the self-assembly of OsBPEI@1 mM Pi–NaCl, and GOx@H_2O. Green circles correspond to frequency changes and red squares to dissipation changes.

Self-assembled colloidal nanoparticles are acquiring an important role in materials science to develop functional materials with molecular-level control. Previously, we have studied the formation of colloidal nanoparticles combining concanavalin A and glucose oxidase, obtaining a supramolecular protein with enzymatic activity.[45] Considering these results, we decided to study the integration of GOx to the supramolecular system already presented. DLS studies of a solution containing the four components (OsBPEI, phosphate, NaCl, and GOx) shows the formation of nanoparticles of 1.5 μm diameter (Fig. 3) and the absence of free GOx molecules (average hydrodynamic diameter 9 nm[45]), indicating that they are incorporated to these particles. Also, there are no essential changes regarding the identical particles in the absence of GOx (see Table 2), suggesting that the incorporation of the enzyme does not affect the colloid structure.

We decided to study these polyelectrolyte-enzyme colloids' electrochemical response and compare their behavior against other systems where OsBPEI was cast from water, 1 M NaCl, and 10 mM phosphate. These combinations were used to modify electrodes using a one-pot strategy, where the different components are left to dry onto the electrode surface at a controlled humidity (30% RH). In all cases, the ratio between the current in the presence and the absence of glucose (j_c/j_0) is higher than 20 (Fig. S4, ESI†).

The best j_c/j_0 ratio is obtained when the solution contains 10 mM phosphate and 1 M NaCl, achieving a value of 45. This increase in the ratio as the system is incorporating different elements can be rationalized as the fact that each component contributes to a better interaction between the polyelectrolyte and the enzyme, NaCl screens local charges and promotes a salting-out effect. At the same time, the phosphate groups act as the crosslinker. However, the current density in the absence of the glucose (0.38 μA cm^{-2}) is similar to a 2 bilayers system built by LbL assembly (Fig. 1A, black circle). This result implies that the colloidal particles are adsorbed on the electrode surface but cannot interact among them to form a thicker layer.

Poly(ethylene glycol) diglycidyl ether (PEDGE) was added to stabilize the modified electrode. This diepoxy compound has

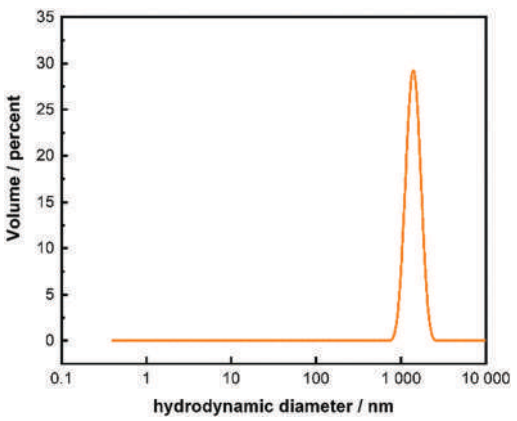

Fig. 3 Particle size distribution obtained by DLS for the system OsBPEI@-GOx,10 mM Pi–NaCl.

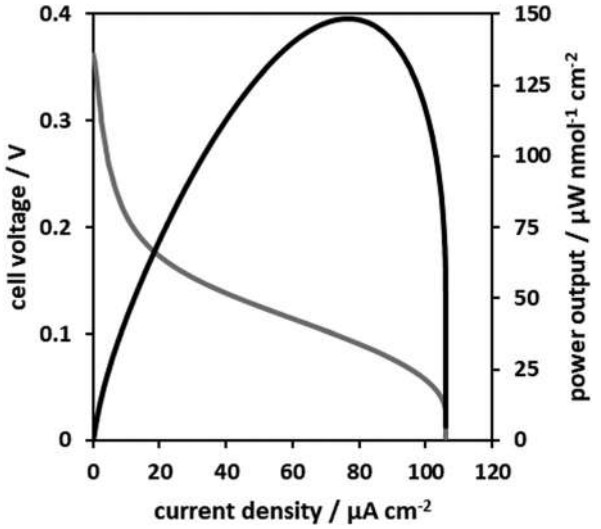

Fig. 4 Cell voltage (gray line) and power output density per nmol of mediator (black line) as a function of the current density in a compartment-less system. An electrode cast from OsBPEI@GOx,10 mM Pi–NaCl-PEDGE was used as bioanode. A high platinum loading gas diffusion electrode was used as the cathode for oxygen reduction.

been widely used to construct electrodes involving enzymes and polyelectrolytes for *in vivo* applications.[46–48] The crosslinker was tested at different concentrations from 0.2 to 1.5 mg mL^{-1}, resulting in 0.8 mg mL^{-1} the best option regarding stability and current response. In this case, the current density in the absence of glucose was 1.3 μA cm^{-2}, representing an increase of more than three times in the amount of osmium; while in the presence of glucose, the catalytic current is 32 μA cm^{-2}, denoting that part of the enzyme is lost, or its interaction with the redox centers is reduced, therefore decreasing the j_c/j_0 ratio. However, it presents a higher catalytic current and a more stable response (see ESI,† Fig. S5 and S6).

Finally, we have evaluated the one-pot stabilized PEGDE electrode as an anode in a biofuel cell. Here, glucose is used as fuel, while oxygen is used as the oxidant in a compartment-less cell. This type of device works at mild conditions (room temperature and neutral pH),[49] allowing to pursuit applications like logic devices[50] and implantable power supplies,[51] including self-powered biosensors.[52] For the oxygen reduction, a high platinum loading gas diffusion electrode was used as the cathode.

Fig. 4 shows the results for the one-pot bioanode at physiological pH, the maximum power output is 148 μW $nmol^{-1}$ cm^{-2} with a maximum current density of 106 μA cm^{-2}, and an open-circuit voltage of 0.36 V. From these results, we can observe that the system presents a behavior according to the reactions involved since the open circuit potential is established by the redox mediator and the oxygen reduction potentials. In Fig. 4, the power output is presented as a function of the nanomoles of mediator since we found that our redox polyelectrolyte yields a maximum power output per nmol of redox centers higher than similar systems[10,48,53–55] (see Table S1, ESI†).

The voltage *vs.* current plot has the typical shape of a fuel cell (Fig. 4, gray line); when current flows, the cell voltage decreases, and the difference between the new voltage and its equilibrium cell voltage is defined as the overpotential. There are three types of overpotential in any fuel cell: activation, ohmic, and concentration overpotentials. Activation overpotential is observed at low currents and related to the finite rate of the electrode's reaction. Ohmic overpotential is observed at intermediate currents, the output voltage practically decays linearly as the current increases, mainly related to the electrolyte conductivity. Concentration overpotential is observed at high currents with a sharp decrease in the voltage output, and it is attributed to the mass transport limitations of the electrochemical reaction.[56] Here, and in the mentioned examples, the concentration overpotential corresponds to the segmental movement of the redox centers and the electron hopping efficiency in the film. In all the cases, the concentration overpotential is the region where the maximum power output is obtained, reinforcing the concept that in our case, the polyamine-phosphate aggregates contribute to the strong interaction among the redox centers, the enzyme, and the electrode surface, delivering a higher output power density.

4 Conclusions

Crosslinked polyelectrolytes have been subject of intensive research due to their key advantages: they are synthesized in mild conditions, they can encapsulate proteins, they can be responsive to external stimuli, their properties can be enhanced by combination with other species or conjugating active molecules to their functional groups.[57] In this work, we use some of these features to generate a redox polymer with a gel-like structure to efficiently mediate the electron transport process between a redox enzyme and an electrode. A condensation reaction between a carbonyl functionalized osmium complex and BPEI was carried out, yielding a redox polymer with a RNH_x : Os ratio of 16 : 1 (where RNH_x represents the different amino moieties present in the polyelectrolyte). This redox polyelectrolyte was dissolved in water, allowing its combination with phosphate as an ionic crosslinker. This combination yields stable colloidal particles, which in the presence of 1 M NaCl can be adsorbed on graphite or gold. The effect of this high salt concentration to facilitate the film growth and the electron transfer mediation can be explained considering the model proposed by Zhang *et al.*[27] regarding the effects of anions on polymer solvation. As a chaotropic anion, chloride ions increase the surface tension around the polyelectrolyte backbone, shifting the equilibrium towards the film formation instead of the redissolution as it happens when phosphate is only present.[35] The results obtained by DLS and QCM-D show that we are in the presence of particles of *ca.* 1 μm diameter, with a high content of water, suggested by the dissipation change by QCM-D. The outstanding electrocatalytic response observed in cyclic voltammetry experiments and its behavior as bioanode considering the power output per nanomol of mediator indicates a strong interaction between the polyelectrolyte and the enzyme to present a fast electron transfer mediation through the film. From these results, we can assume regions with hydrophobic

assemblies containing the polyelectrolyte and the enzyme in close contact within a gel-like structure, allowing the redox centers' segmental motion to facilitate the electron transfer process throughout the film.

As an application, a fuel cell was constructed where the microgel was stabilized with PEDGE. As the redox polyelectrolyte-GOx assembly presents a fast electron transfer in all its steps, the power output obtained per mass unit surpass previous results reported in the literature. Electrochemical based energy storage devices still face enormous challenges to become everyday products.[58] The results presented here based on the use of an ionically crosslinked redox polyelectrolyte, where moieties as osmium complexes or enzymes like glucose oxidase can be easily replaced, opens a new route to tackle challenges referring electron transport and power density in electrochemical devices.

Conflicts of interest

There are no conflicts to declare.

Acknowledgements

L. L. C. O. thanks a scholarship of CONICET (Argentina). M. L. C., O. A. and F. B. are research staff of CONICET (Argentina). Universidad de Buenos Aires (UBACYT 20020170100341BA), ANPCYT (BID PICT 2015-0801, BID PICT 2016-1680, BID PICT 2017-1523) and CONICET (PIP-0370) are acknowledged for financial support.

References

1 P. G. Lawrence and Y. Lapitsky, *Langmuir*, 2015, **31**, 1564–1574.
2 S. E. Herrera, M. L. Agazzi, M. L. Cortez, W. A. Marmisollé, M. Tagliazucchi and O. Azzaroni, *ChemPhysChem*, 2019, **20**, 1044–1053.
3 H. Jonassen, A.-L. Kjøniksen and M. Hiorth, *Biomacromolecules*, 2012, **13**, 3747–3756.
4 P. Andreozzi, E. Diamanti, K. R. Py-Daniel, P. R. Cáceres-Vélez, C. Martinelli, N. Politakos, A. Escobar, M. Muzi-Falconi, R. Azevedo and S. E. Moya, *ACS Appl. Mater. Interfaces*, 2017, **9**, 38242–38254.
5 M. L. Agazzi, S. E. Herrera, M. L. Cortez, W. A. Marmisollé and O. Azzaroni, *Colloids Surf., B*, 2020, **190**, 110895.
6 S. E. Herrera, M. L. Agazzi, M. L. Cortez, W. A. Marmisollé, M. Tagliazucchi and O. Azzaroni, *Chem. Commun.*, 2019, **55**, 14653–14656.
7 J. J. Virgen-Ortíz, J. C. S. dos Santos, Á. Berenguer-Murcia, O. Barbosa, R. C. Rodrigues and R. Fernandez-Lafuente, *J. Mater. Chem. B*, 2017, **5**, 7461–7490.
8 D. R. Holycross and M. Chai, *Macromolecules*, 2013, **46**, 6891–6897.
9 S. Kobayashi, *Prog. Polym. Sci.*, 1990, **15**, 751–823.
10 N. P. Godman, J. L. DeLuca, S. R. McCollum, D. W. Schmidtke and D. T. Glatzhofer, *Langmuir*, 2016, **32**, 3541–3551.
11 S. A. Merchant, D. T. Glatzhofer and D. W. Schmidtke, *Langmuir*, 2007, **23**, 11295–11302.
12 R. D. Milton, F. Giroud, A. E. Thumser, S. D. Minteer and R. C. T. Slade, *Electrochim. Acta*, 2014, **140**, 59–64.
13 J. M. Díaz-González, R. A. Escalona-Villalpando, L. G. Arriaga, S. D. Minteer and J. R. Casanova-Moreno, *Electrochim. Acta*, 2020, **337**, 135782.
14 J.-Y. Wang, L.-C. Chen and K.-C. Ho, *ACS Appl. Mater. Interfaces*, 2013, **5**, 7852–7861.
15 Y.-M. Yan, I. Baravik, O. Yehezkeli and I. Willner, *J. Phys. Chem. C*, 2008, **112**, 17883–17888.
16 T. Bahar and M. S. Yazici, *Asia-Pac. J. Chem. Eng.*, 2018, **13**, 1–9.
17 D. Brondani, B. de Souza, B. S. Souza, A. Neves and I. C. Vieira, *Biosens. Bioelectron.*, 2013, **42**, 242–247.
18 A. vander Straeten, A. Bratek-Skicki, A. M. Jonas, C.-A. Fustin and C. Dupont-Gillain, *ACS Nano*, 2018, **12**, 8372–8381.
19 A. Rodriguez-Abetxuko, D. Sánchez-deAlcázar, A. L. Cortajarena and A. Beloqui, *Adv. Mater. Interfaces*, 2019, 1900598.
20 D. Zappi, L. L. Coria-Oriundo, E. Piccinini, M. Gramajo, C. von Bilderling, L. I. Pietrasanta, O. Azzaroni and F. Battaglini, *Phys. Chem. Chem. Phys.*, 2019, **21**, 22947–22954.
21 E. M. Kober, J. V. Caspar, B. P. Sullivan, E. M. Kober, J. V. Caspar, B. Patrick Sullivan and T. J. Meyer, *Inorg. Chem.*, 1988, **27**, 4587–4598.
22 C. Danilowicz, E. Cortón and F. Battaglini, *J. Electroanal. Chem.*, 1998, **445**, 89–94.
23 I. Boron, S. Wirth and F. Battaglini, *Electroanalysis*, 2017, **29**, 616–621.
24 G. Priano, G. González, M. Günther and F. Battaglini, *Electroanalysis*, 2008, **20**, 91–97.
25 M. L. Cortez, A. L. Cukierman and F. Battaglini, *Electrochem. commun.*, 2009, **11**, 990–993.
26 C. J. B. van Treslong and A. J. Staverman, *Recl. Trav. Chim. Pays Bas.*, 1974, **93**, 171–178.
27 Y. Zhang, S. Furyk, D. E. Bergbreiter and P. S. Cremer, *J. Am. Chem. Soc.*, 2005, **127**, 14505–14510.
28 Y. Huang and Y. Lapitsky, *Biomacromolecules*, 2012, **13**, 3868–3876.
29 Y. Huang and Y. Lapitsky, *Langmuir*, 2011, **27**, 10392–10399.
30 B. D. Coday, T. Luxbacher, A. E. Childress, N. Almaraz, P. Xu and T. Y. Cath, *J. Membr. Sci.*, 2015, **478**, 58–64.
31 A. Dukhin, S. Dukhin and P. Goetz, *Langmuir*, 2005, **21**, 9990–9997.
32 D. Beaglehole, B. Webster and S. Werner, *J. Colloid Interface Sci.*, 1998, **202**, 541–550.
33 M. L. Cortez, A. Lorenzo, W. Marmisollé, C. von Bilderling, E. Maza, L. I. Pietrasanta, F. Battaglini, M. Ceolín and O. Azzaroni, *Soft Matter*, 2018, **14**, 1939–1952.
34 L. Venkataraman, J. E. Klare, I. W. Tam and C. Nuckolls, *Nano Lett.*, 2006, **6**, 458–462.
35 G. Laucirica, W. A. Marmisollé and O. Azzaroni, *Phys. Chem. Chem. Phys.*, 2017, **19**, 8612–8620.
36 W. J. Dressick, K. J. Wahl, N. D. Bassim, R. M. Stroud and D. Y. Petrovykh, *Langmuir*, 2012, **28**, 15831–15843.

37 J. Irigoyen, S. E. Moya, J. J. Iturri, I. Llarena, O. Azzaroni and E. Donath, *Langmuir*, 2009, **25**, 3374–3380.
38 G. Laucirica, G. Pérez-Mitta, M. E. Toimil-Molares, C. Trautmann, W. A. Marmisollé and O. Azzaroni, *J. Phys. Chem. C*, 2019, **123**, 28997–29007.
39 G. Pérez-Mitta, W. A. Marmisollé, A. G. Albesa, M. E. Toimil-Molares, C. Trautmann and O. Azzaroni, *Small*, 2018, **14**, 1702131.
40 E. J. Calvo, R. Etchenique, L. I. Pietrasanta, A. Wolosiuk and C. Danilowicz, *Anal. Chem.*, 2001, **73**, 1161–1168.
41 D. A. Capdevila, W. A. Marmisollé, F. J. Williams and D. H. Murgida, *Phys. Chem. Chem. Phys.*, 2013, **15**, 5386–5394.
42 C. Peng, J. Liu, Y. Xie and J. Zhou, *Phys. Chem. Chem. Phys.*, 2016, **18**, 9979–9989.
43 M. Gruber, P. Greisen, C. M. Junker and C. Hélix-Nielsen, *J. Phys. Chem. B*, 2014, **118**, 1207–1215.
44 P. G. Lawrence and Y. Lapitsky, *Langmuir*, 2015, **31**, 1564–1574.
45 E. Piccinini, D. Pallarola, F. Battaglini and O. Azzaroni, *Chem. Commun.*, 2015, **51**, 14754–14757.
46 M. Cadet, S. Gounel, C. Stines-Chaumeil, X. Brilland, J. Rouhana, F. Louerat and N. Mano, *Biosens. Bioelectron.*, 2016, **83**, 60–67.
47 N. Vasylieva, B. Barnych, A. Meiller, C. Maucler, L. Pollegioni, J. S. Lin, D. Barbier and S. Marinesco, *Biosens. Bioelectron.*, 2011, **26**, 3993–4000.
48 F. Conzuelo, N. Marković, A. Ruff and W. Schuhmann, *Angew. Chem., Int. Ed.*, 2018, **57**, 13681–13685.
49 M. T. Meredith and S. D. Minteer, *Annu. Rev. Anal. Chem.*, 2012, **5**, 157–179.
50 E. Katz, *Signal-switchable electrochemical systems: materials, methods, and applications*, Wiley, Weinheim, Germany, 2018.
51 M. Gamella, A. Koushanpour and E. Katz, *Bioelectrochemistry*, 2018, **119**, 33–42.
52 L. Sun, X. Zhang, W. Wang and J. Chen, *Anal. Methods*, 2015, **7**, 5060–5066.
53 D. P. Hickey, F. Giroud, D. W. Schmidtke, D. T. Glatzhofer and S. D. Minteer, *ACS Catal.*, 2013, **3**, 2729–2737.
54 J. Liu, X. Zhang, H. Pang, B. Liu, Q. Zou and J. Chen, *Biosens. Bioelectron.*, 2012, **31**, 170–175.
55 Z. Zhong, L. Qian, Y. Tan, G. Wang, L. Yang, C. Hou and A. Liu, *J. Electroanal. Chem.*, 2018, **823**, 723–729.
56 G. T. R. Palmore, in *Bioelectrochemistry*, ed. P. N. Bartlett, John Wiley & Sons, Ltd, Chichester, UK, 2008, pp. 359–375.
57 Y. Lapitsky, *Curr. Opin. Colloid Interface Sci.*, 2014, **19**, 122–130.
58 X. Xiao, H. Xia, R. Wu, L. Bai, L. Yan, E. Magner, S. Cosnier, E. Lojou, Z. Zhu and A. Liu, *Chem. Rev.*, 2019, **119**, 9509–9558.

